Título artículo / Títol article:	Electrophoretic deposition of nanostructured-TiO2/ chitosan composite coatings on stainless Steel
Autores / Autors	L. Cordero Arias, S. Cabanas Polo, Haoxiang Gao, J. Gilabert, E. Sanchez, J. A. Roether, D. W. Schubert, S. Virtanene and A. R. Boccaccinia
Revista:	RSC Advances., 2013, 3
Versión / Versió:	Postprint de l'autor
Cita bibliográfica / Cita bibliogràfica (ISO 690):	Cordero-Arias L., Cabanas-Polo S., Gao H. X. , Gilabert J., Sanchez E., Roether J., Schubert D., Virtanen S. and Boccaccini A. R. : 'Electrophoretic deposition of nanostructured TiO_2/chitosan composite coatings on stainless steel', RSC Adv., 2013, **3**, 11247-11254.
url Repositori UJI:	http://hdl.handle.net/10234/83549

RSC Advances

RSC Publishing

PAPER

View Article Online
View Journal

Electrophoretic deposition of nanostructured-TiO_2/chitosan composite coatings on stainless steel

Cite this: DOI: 10.1039/c3ra40535d

L. Cordero-Arias,[a] S. Cabanas-Polo,[a] Haoxiang Gao,[b] J. Gilabert,[c] E. Sanchez,[c] J. A. Roether,[d] D. W. Schubert,[d] S. Virtanen[e] and A. R. Boccaccini[a]

Received 30th January 2013,
Accepted 4th March 2013

DOI: 10.1039/c3ra40535d

www.rsc.org/advances

Novel chitosan composite coatings containing titania nanoparticles (n-TiO_2) for biomedical applications were developed by electrophoretic deposition (EPD) from ethanol–water suspensions. The optimal ethanol–water ratio was studied in order to avoid bubble formation during the EPD process and to ensure homogeneous coatings. Different n-TiO_2 contents (0.5–10 g L^{-1}) were studied for a fixed chitosan concentration (0.5 g L^{-1}) and the properties of the electrophoretic coatings obtained were characterized. Coating composition was analyzed by thermogravimetric analysis (TG), Fourier transform infrared spectroscopy (FTIR) and X-ray diffraction (XRD) analysis. Scanning electron microscopy (SEM) was employed to study both the surface and the cross section morphology of the coatings, and the thicknesses (2–6 μm) of the obtained coatings were correlated with the initial ceramic content. Contact angle measurements, as a preliminary study to predict hypothetic protein attachment on the coatings, were performed for different samples and the influence of a second chitosan layer on top of the coatings was also tested. Finally, the electrochemical behavior of the coatings, evaluated by polarization curves in DMEM at 37 °C, was studied in order to assess the corrosion resistance provided by the n-TiO_2/chitosan coatings.

Introduction

Titania (TiO_2) is a biocompatible ceramic material being used to develop biomedical coatings sometimes also in combination with hydroxyapatite.[1–7] Titania has a proven biocompatibility[5,8–10] and it can enhance the implant integration with host tissue when used in bone tissue replacement applications.[11–14] Titania also presents antibacterial properties, which increases its possible benefits in the biomedical field.[15–17]

Numerous techniques are employed to produce TiO_2 coatings on metallic surfaces, such as plasma spray technique,[18,19] micro-arc oxidation (MAO),[4] sol–gel[20] or electrophoretic deposition (EPD).[1,3,21,22] EPD emerges as a versatile, simple and low cost technique to create highly homogeneous coatings with some advantages, like the possibility to deposit materials on 3D structures as well as on porous materials, *e.g.* scaffolds.[17,23–27]

EPD is a deposition technique suitable to produce a wide variety of coatings due to the possibility of applying different types of materials and combination of materials, *e.g.* inorganic, polymeric and composite materials.[17,23,26,27] This technique uses an electric field applied between two electrodes immersed into a colloidal suspension.[23,26] The electric field imparts electrophoretic motion to charged particles in suspension causing their movement to the oppositely charged electrode, where they deposit forming a coating over it. EPD of TiO_2 has been carried out using different solvents, mainly acetylacetone and acetone,[28–31] but water and water–ethanol mixtures have also been used in a reduced scale.[3,32–35]

Ceramic deposits obtained by EPD require a sintering process at high temperature to achieve high density materials. To avoid this sintering step, which can lead to possible degradation and microstructural damage of the coating, *e.g.* phase changes and dilatation/contractions due to the thermal cycle, a convenient approach is being considered for biomedical applications: the addition of polymers in combination with the ceramic components effectively forming organic–inorganic composite coatings.[17,36] These soft composite coatings also offer the advantage of providing a better connection between the rigid implant and the vascularized ''softer'' bone tissue, reducing the large elastic mismatch at the interface.[36–38] In the case of EPD a large family of this type of organic–inorganic coatings has been produced, as reviewed elsewhere.[17] An interesting polymer for this purpose is chitosan,[39–41] which

[a]Institute of Biomaterials (WW7), Department of Materials Science and Engineering, University of Erlangen-Nuremberg, Cauerstrasse 6, D-91058 Erlangen, Germany
[b]Department of Materials, Imperial College London, South Kensington Campus, London SW7 2AZ, United Kingdom
[c]Institute of Ceramic Technology (ITC), University Jaume I, Avenida Vicent SosBaynat, 12006-Castellon, Spain
[d]Institute of Polymer Materials, Department of Materials Science and Engineering, University of Erlangen-Nuremberg, Martensstrasse 7, D-91058 Erlangen, Germany
[e]Institute for Surface Science and Corrosion (LKO, WW4), Department of Materials Science and Engineering, University of Erlangen-Nuremberg, Martensstrasse 7, D-91058 Erlangen, Germany

has been already widely used in combination with EPD to produce a variety of bioactive coatings.[42–49] This polymer is a natural cationic polysaccharide which is made from alkaline *N*-deacetylation of chitin[40,41] and has a proven biocompatibility, also exhibiting antibacterial activity, film forming ability and drug delivery potential.[50–52]

The aim of this research was to develop a new group of electrophoretic chitosan-based coatings on stainless steel substrates incorporating, for the first time, TiO_2 nanoparticles as an inorganic phase. The deposition conditions (concentration, potential and deposition time) as well as the colloidal stability of the starting suspensions were investigated. The coating composition was studied using XRD, FTIR and TG-DTA techniques. The electrochemical behavior was also evaluated by polarization curves of the coatings to assess the effect of the new coatings on the corrosion behaviour of the stainless steel substrates.

Materials and methods

Chitosan (80 kDa, 85% deacetilation, Sigma), nanometer titania powder (TiO_2) (21 nm particle size, P25, Evonik Industries), water and ethanol were used as-received to prepare stable suspensions suitable to be used for EPD. A constant concentration of 0.5 g L^{-1} chitosan (prepared using 1 vol.% of acetic acid) was used according to the results reported by other authors.[46,47,53] TiO_2 concentration was varied from 0.5 to 10 g L^{-1}. In order to avoid hydrogen bubbles formation during the EPD process (due to water electrolysis) different ethanol–water ratios were considered. All suspensions prepared were magnetically stirred for 5 min followed by 30 min of ultrasonication and subsequent 5 min of magnetic stirring, in order to guarantee an adequate dispersion of the components in the suspension. The colloidal stability of the suspension was analyzed by means of ζ-potential measurements using a Zetasizer nano ZS equipment (Malvern Instruments, UK).

Stainless steel AISI 316L electrodes (plates of 2.25 cm^2 deposition area) were used to deposit the n-TiO_2/chitosan composite coating *via* constant voltage EPD. The distance between the electrodes in the EPD cell was kept constant at 10 mm. Deposition voltages and times in the ranges of 2–50 V and 15 s to 5 min, respectively, were studied. Deposition yield was evaluated using an analytical balance (precision 0.0001 g). Coated substrates were dried during 24 h in normal air at room temperature prior to mass determination.

In order to characterize the coatings, XRD (D8 Advance Bruker, Germany), FTIR (Bruker Instruments, Germany), as well as thermogravimetric (TG) and differential thermal analysis (DTA) (TGA/SDTA 851e, Mettler) tests were performed. In this last technique, the tests were carried out using a dynamic air atmosphere, a heating rate of 10 °C min^{-1} and applying a maximum temperature of 800 °C. The surface microstructures of the coatings were analyzed by scanning electron microscopy (SEM) (LEO 435VP, Zeiss Leica). The contact angle was measured (DSA30 Kruess GmbH, Germany) using deionized water droplets to evaluate the wettability of the coatings, since this property is determinant for the initial protein attachment, relevant for the intended biomedical applications in bone replacement devices.

The electrochemical behavior of the coatings was also studied in order to test their possible protective properties. Potentiodynamic polarization curves were carried out using a potentiostat/galvanostat Autolab PGSTAT 30. The samples were immersed in 100 mL of Dulbecco's MEM (DMEM, Biochrom) at 37 °C. A conventional three-electrode system was used, where a platinum foil served as counter electrode and Ag/AgCl (3 mol dm^{-3} KCl) was used as reference electrode. The analysis was carried out using an O-ring cell with an exposed sample area of 0.38 cm^2 with a potential sweep rate of 1 mV s^{-1}.

Results and analysis

Suspension stability and electrophoretic deposition

It is well known that water electrolysis during the EPD process has a negative effect on the homogeneity and adhesion of the as-obtained coatings due to the generation of gas bubbles.[27] Ethanol–water mixtures have been proven to provide a better stabilization of polymer/inorganic particle mixtures in comparison with other water-based solutions.[44,45] In order to avoid microstructural inhomogeneities in the coating and to obtain highly stabilized suspensions, different ethanol–water ratios (up to 95 vol.% ethanol) were tested, while the chitosan and n-TiO_2 concentration were kept constant (0.5 and 10 g L^{-1}, respectively). Solutions with ethanol–water ratio of 80 : 20 were found to be the most stable ones. Only after 192 h of aging, a slight sedimentation was observed (Fig. 1). Zeta potential of a suspension prepared with the same ethanol–

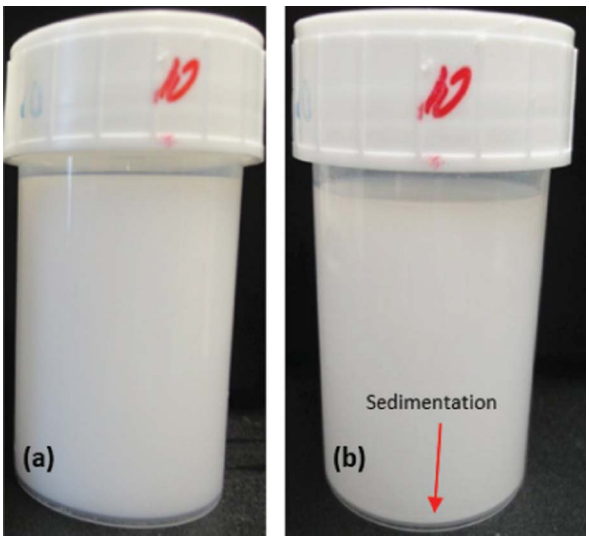

Fig. 1 Stability of n-TiO_2/chitosan suspensions in ethanol–water (80 : 20) solvent at 0 h (a) and 192 h (b) after preparation.

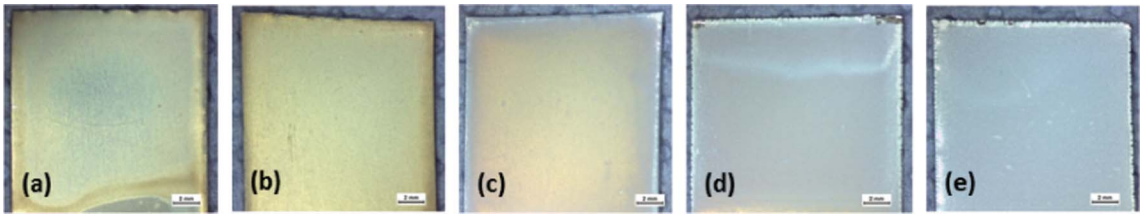

Fig. 2 Electrophoretic n-TiO_2/chitosan coatings produced with 0.5 g L^{-1} chitosan suspensions in ethanol–water solvent and different concentrations of n-TiO_2 using a voltage of 25 V and a deposition time of 1 min (n-TiO_2 appears as a white area in the coatings). (a) 0.5, (b) 1.5, (c) 3, (d) 6 and (e) 10 g L^{-1} n-TiO_2. (Scale bar: 2 mm)

water ratio, where the n-TiO_2 concentration was decreased to 0.1 g L^{-1} in order to ensure a reliable measurement, was found to be 82 ± 21 mV. This relatively high zeta potential value evidences the high stability of the suspension and also predicts a cathodic deposition, indicating that the suspension is suitable for EPD.

Homogeneous and crack-free electrophoretic coatings were obtained for voltages in the range 20–30 V and for deposition times between 0.5 and 1.5 min. Voltage of 25 V and deposition time of 1 min were chosen to study the influence of the n-TiO_2 concentration on coating quality. Fig. 2 shows images of the different coatings obtained with varying n-TiO_2 content from 0.5 to 10 g L^{-1}. As it can be observed, homogeneous coatings are obtained for all n-TiO_2 concentrations. As expected, the higher the n-TiO_2 concentration in suspension, the higher the n-TiO_2 content in the coatings. This tendency is also observed in Fig. 3 where a linear behavior between n-TiO_2 concentration and deposition mass is obtained.

Fig. 4 shows the surface morphology for four different coatings prepared with different n-TiO_2 concentrations (1.5, 3, 6 and 10 g L^{-1}). As it can be observed, the sample prepared using a suspension with 1.5 g L^{-1} n-TiO_2 (Fig. 4a) presents a homogenous surface which is free of cracks. When the titania concentration is increased up to 3 g L^{-1} (Fig. 4b), a higher tendency of the titania nanoparticles to agglomerate is observed and, consequently, larger clusters (20–40 μm) are obtained. However, this coating also presents a homogenous surface free of cracks or any other defects. The coatings produced with higher titania contents (6 and 10 g L^{-1}, Fig. 4c and 4d, respectively) show an important accumulation of cracks, with widths of around 1–2 μm. The higher concentration of n-TiO_2 in these samples decreases the proportion of chitosan within the coating and, therefore, the coatings become more brittle and susceptible of microcracking due to internal stresses developed during the drying process. This effect is also observed when the samples are subjected to deformation by bending to approximately 180° (Fig. 5). As the content of titania within the coatings increases, a higher number of cracks, that propagate from the edges to the center of the coating, is observed (Fig. 5b–5d). In the case of samples prepared with suspensions containing 6 and 10 g L^{-1} n-TiO_2, detachment of the coatings can also be seen. However, for the sample obtained with 1.5 g L^{-1} n-TiO_2 a qualitative good adhesion of the coating is observed after deformation of the substrate by bending and only a few cracks appear at the edges, probably due to the higher ceramic accumulation at these points during the EPD process. These simple observations are important to infer the best possible n-TiO_2 concentration in the coatings that will lead to homogeneous coatings firmly adhered to the substrate and free of drying microcracks, which are also sufficiently compliant to sustain

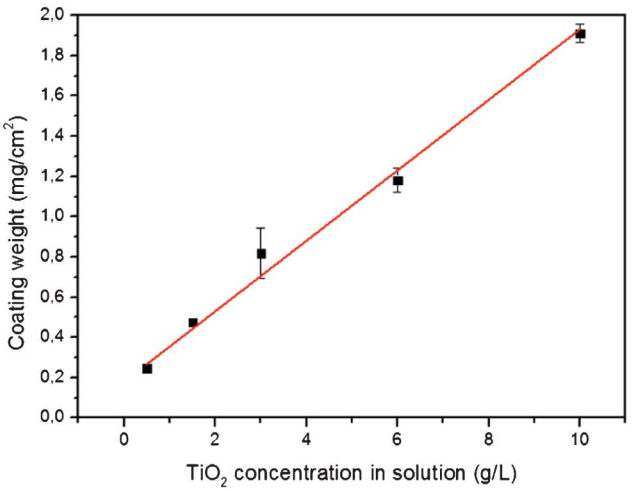

Fig. 3 Relationship between n-TiO_2 concentration in solution and deposited mass per area using 0.5 g L^{-1} chitosan suspensions in ethanol–water solvent. Deposition potential: 25 V and deposition time: 1 min.

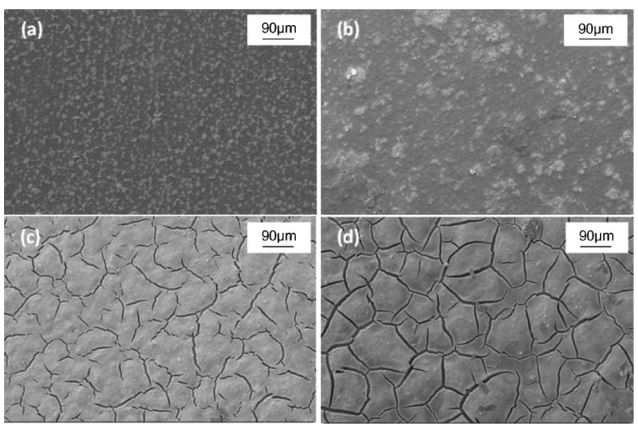

Fig. 4 SEM images of coating surfaces produced by EPD from solutions with different n-TiO_2 contents: 1.5 (a), 3 (b), 6 (c) and 10 g L^{-1} (d). Lighter areas in (a) and (b) represent n-TiO_2 clusters visible on the surface of the coatings.

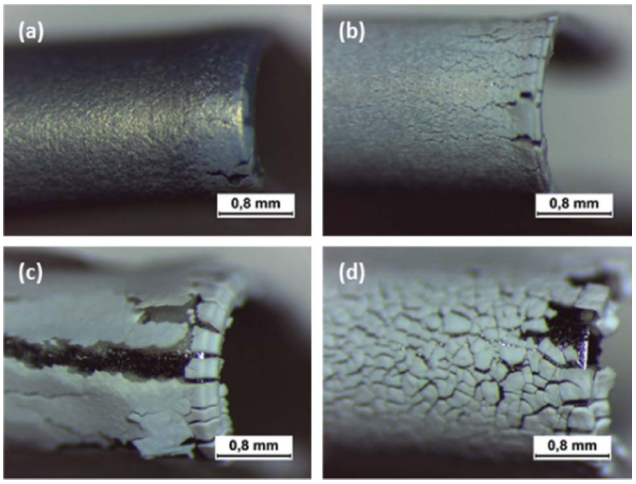

Fig. 5 Bent n-TiO_2/chitosan coatings produced by EPD with 0.5 g L^{-1} chitosan suspensions in ethanol–water solvent and different concentrations of n-TiO_2 using voltage of 25 V and deposition time of 1 min (n-TiO_2 appears as a white area in the images). (a) 1.5, (b) 3, (c) 6 and (d) 10 g L^{-1} n-TiO_2.

damage by possible impact loads or deformation of the substrate during handling.

The morphologies of the cross section of the coatings obtained with n-TiO_2 concentrations of 1.5 and 10 g L^{-1} are shown in Fig. 6. The thickness of the coating prepared with 1.5 g L^{-1} n-TiO_2 suspensions is around 2 μm (Fig. 6a) and, as expected from Fig. 3 where it was shown that the higher the ceramic particles concentration, the higher the deposition rate, the coating prepared with 10 g L^{-1} n-TiO_2 suspension presents a higher thickness of around 5–6 μm (Fig. 6c). In both cases, the coatings appear to be dense, fairly homogenous in microstructure and rather uniform in their thickness.

Wetting behavior

As it is well known, both a too high hydrophilicity as well as a too high hydrophobicity in biomaterials intended for bone tissue regeneration are not desired since the extent of critical

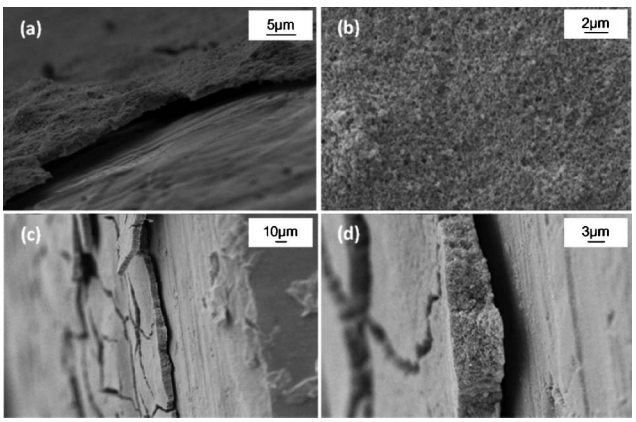

Fig. 6 SEM images of coatings cross sections. Coatings were obtained by EPD using 1.5 (a and b) and 10 g L^{-1} (c and d) n-TiO_2 concentration in the suspension.

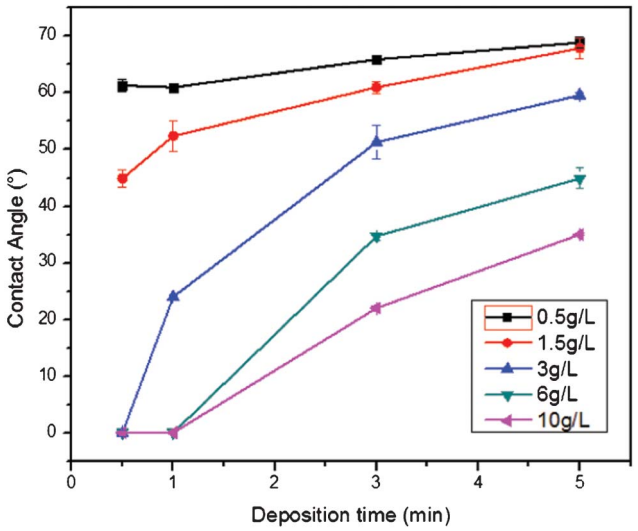

Fig. 7 Contact angle for coatings obtained from suspensions with different n-TiO_2 content (0.5, 1.5, 3, 6 and 10 g L^{-1}) as a function of deposition time (0.5, 1, 3 and 5 min) of the second chitosan layer (produced by EPD with a voltage of 15 V from a solution with 0.5 g L^{-1} chitosan). (3 samples were measured for each condition).

protein attachment to the surface can be negatively affected.[54] According to Menzies and Jones,[54] an ideal contact angle for bone regenerative applications should be between 35° and 80°, while Lee *et al.*[55] consider that 55° is the optimal value to improve blood serum protein adsorption. In the present n-TiO_2/chitosan composite coatings the wetting angle can be tailored by varying the relative content of chitosan and n-TiO_2. In principle, these n-TiO_2/chitosan coatings present high hydrophilicity. In order to increase the contact angle value, it is possible to deposit a second chitosan layer on top of the n-TiO_2/chitosan composite coating. In this study, this layer was also developed by EPD using an applied voltage of 15 V and a 0.5 g L^{-1} chitosan solution prepared in 1 vol.% acetic acid solution.

Fig. 7 shows the contact angle measurements as a function of the deposition time for coatings with different n-TiO_2 contents.

From Fig. 7 it can be observed that the coating obtained with the 0.5 g L^{-1} n-TiO_2 suspension presents a contact angle of 61° even with just 0.5 min of deposition, increasing to 69° after 5 min of EPD. In the case of coatings prepared with 1.5 g L^{-1} n-TiO_2 suspension, the contact angle increases from 45° to 68° for the analyzed deposition times. These relatively high contact angle values are due to the presence of chitosan on the sample and the relatively low content of titania in those coatings. The effect of n-TiO_2 on the wettability of composite films can be appreciated when the n-TiO_2 content is increased in the different suspensions. The higher the titania content, the higher the wettability. According to the contact angle criteria mentioned above,[54,55] the coatings prepared from 0.5 and 1.5 g L^{-1} n-TiO_2 suspensions should exhibit the best protein attachment behavior for bone replacement applications, since the measured contact angle is always within the recommended range of 35–80° and close to the optimal value

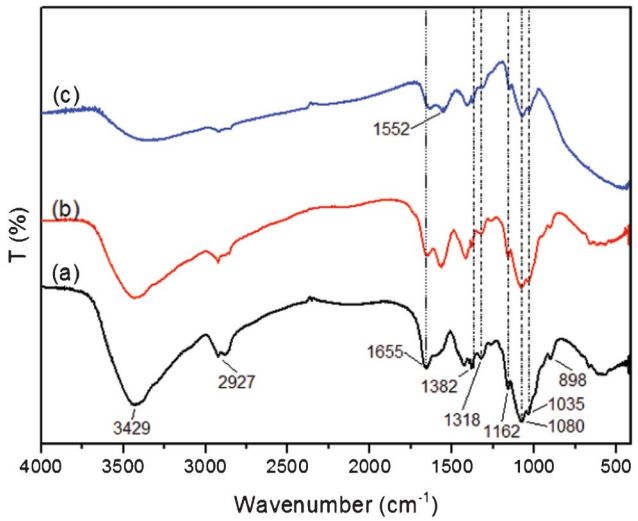

Fig. 8 FTIR results for the pure chitosan powder (a), pure chitosan coating (b) and 1.5 g L^{-1} TiO_2/chitosan coating (c).

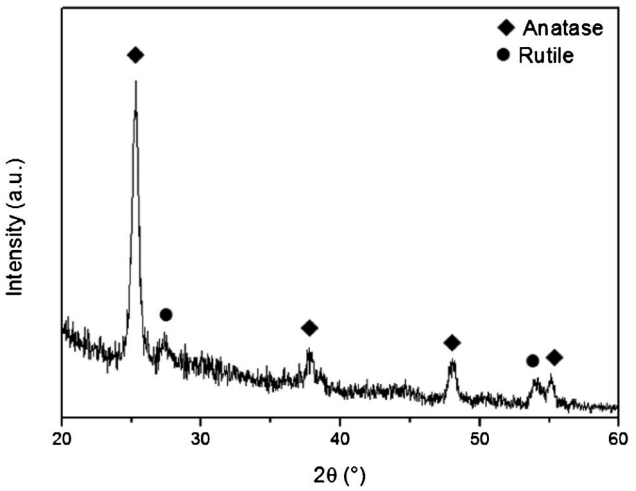

Fig. 9 XRD results of a n-TiO_2-chitosan coating on stainless steel obtained from a 1.5 g L^{-1} n-TiO_2 suspension. The diffractogram confirms the presence of anatase and rutile which correspond to the commercial n-TiO_2 material used (P25).

of 55°. After 3 min of deposition, the coatings with a higher content of titania (3 and 6 g L^{-1}) also present an acceptable contact angle, especially the coating obtained using the 3 g L^{-1} n-TiO_2 suspension. On the other hand, the coating fabricated with 10 g L^{-1} n-TiO_2 suspension shows the lowest contact angle values, reaching its maximum (35°) after 5 min of deposition. It is important to mention that the contact angles for the coatings, especially those obtained from the 6 and 10 g L^{-1} n-TiO_2 suspensions, are also affected by the presence of cracks developed during the drying process (see Fig. 4).

Analysis of the coating composition and structure

The coatings composition was analyzed by means of FTIR and XRD techniques. The FTIR results for pure chitosan powder, a pure chitosan coating and a n-TiO_2/chitosan composite coating prepared with a titania concentration of 1.5 g L^{-1} can be observed in Fig. 8.

For pure chitosan (both in powder form and as a coating) two different peaks at 898 and 1162 cm^{-1} can be observed which are associated to the –C–O–C– group vibration of saccharides.[56–59] In the case of n-TiO_2/chitosan composite coating, the peak at 1162 cm^{-1} is also observed but the one at 898 cm^{-1} is overlapped with a broad band which extends up to 400 cm^{-1}. The peaks at 1035 and 1080 cm^{-1} can be attributed to the C–O stretching vibration of the chitosan,[56–60] while the ones at 1655, 1552 and 1318 cm^{-1} are assigned to the N–H bending of the amines groups I and II, respectively.[56–60] The symmetric deformation mode of the CH_3 group appears at 1382 cm^{-1} and the stretching one for C–H bond at 2925 cm^{-1}. Finally, the broad band at approximately 3429 cm^{-1} corresponds to the O–H stretching vibration of chitosan.[56–60] As mentioned above, in the case of n-TiO_2/chitosan composite coating, there is a broad band that extends below 950 cm^{-1} (and up to 400 cm^{-1}) which can be associated to the presence of titania in the coating.[21,61,62] In order to further corroborate the presence of the ceramic phase within the composite coating, X-ray diffraction analyses were carried out. Fig. 9 shows the X-ray diffractogram of the n-TiO_2/chitosan composite coating prepared with 1.5 g L^{-1} n-TiO_2 suspension where the peaks corresponding to both the anatase (2θ = 25.22°, 37.74°, 47.95°) and the rutile (2θ = 27.37°, 35.99°, 54.26°) crystalline phases of titanium dioxide are observed.[21,63]

Thermal properties

The thermal behavior of three different samples (1.5, 3 and 10 g L^{-1} n-TiO_2) was characterized by TG and DTA techniques (Fig. 10). The first mass loss observed in the TG curve in the range of 25–150 °C can be attributed to the physically adsorbed water that was retained in the coating structure. Between 200 and 550 °C an important change of mass associated with an exothermic peak in the DTA curves appears in all coatings, which can be attributed to the combustion reaction of the chitosan.[46] The total mass loss for the coatings made from 10,

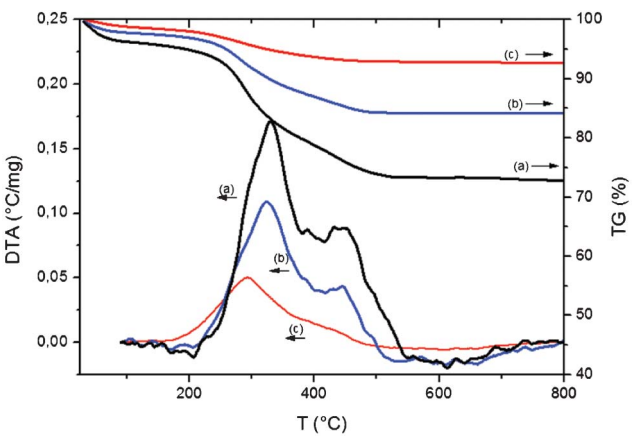

Fig. 10 TG and DTA results of the tests performed on the coatings produced from EPD solutions with initial n-TiO_2 concentrations of 1.5 (a), 3 (b) and 10 g L^{-1} (c).

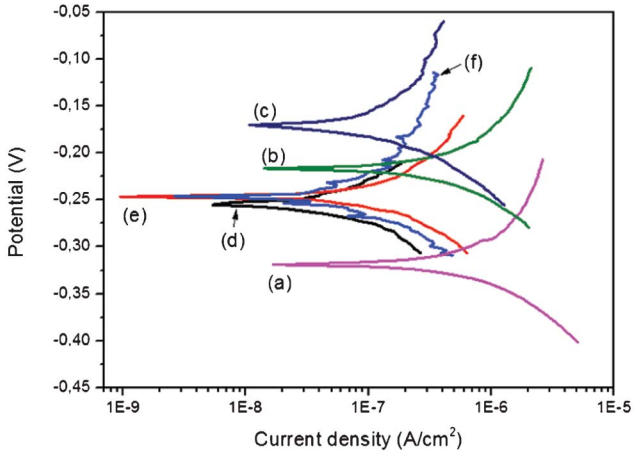

Fig. 11 Polarization curves obtained using DMEM at 37 °C of the bare stainless steel substrate (a), n-TiO_2/chitosan coatings produced from the n-TiO_2 solutions with 3 (b) and 6 g L^{-1} (c), and coatings produced from n-TiO_2 solutions with 1.5 (d), 3 (e) and 6 g L^{-1} (f) with a second chitosan layer.

3 and 1.5 g L^{-1} n-TiO_2 suspensions were found to be 7, 16 and 27%, respectively, of which 5, 13 and 23% corresponded to the chitosan contribution. These results are in good agreement with the amount of chitosan in the initial suspensions (5, 14 and 25 wt.% chitosan, respectively). Regarding the DTA curves, it is observed that the main peak, which corresponds to the chitosan combustion, shifts to the low temperature side and it is less intense with increasing titania content. This thermal behaviour appears frequently due to the fact that in samples with higher chitosan content the peak signal is more defined and a higher temperature is needed to burn out the chitosan completely. Once the chitosan is burned out (above 550 °C), there is no other important change in the mass loss, therefore, it can be concluded that the residual material in the coating is titania. According to the TG curves, the final ceramic contents (wt.%) were 93, 84 and 73% for the coatings prepared with 10, 3 and 1.5 g L^{-1} n-TiO_2 suspensions, respectively. These values are relatively high for the inorganic component in this type of coating and confirm the suitability of EPD for developing composite coatings for biomedical applications where a high content of the inorganic filler may be desired to impart bioactivity.

Electrochemical behavior

The corrosion resistance of metallic materials used in biological environments is one of the key parameters determining their success. Applying a protective coating is one of the alternatives to tackle the relatively low corrosion resistance of stainless steel in biological fluids, which is due to the high chloride content in biological fluids. Fig. 11 presents the polarization curves of the uncoated 316 L (bare metal) and of coated substrates prepared from suspensions with different n-TiO_2 concentrations. Also, polarization curves for coatings which were covered with a second layer of chitosan are presented. It can be observed that all coatings show a higher E_{corr} and a lower i_{corr} compared to the bare metal, meaning that the n-TiO_2/chitosan composite coatings protect the substrate. In the case of using a single TiO_2/chitosan composite layer, the corrosion potential increases with the amount of titania due to a barrier effect that these particles produced, reducing i) the direct contact of DMEM with the surface of the substrate and ii) the tendency of the system to be corroded. However, the addition of a second chitosan layer seems to control the electrochemical behavior of the coatings, considering that, independently of the ceramic content of the first layer, all coatings have a similar corrosion potential and current density. The chitosan layer decreases significantly the current density from 1065 nA cm^{-2} (bare metal) to a mean value of 215 nA cm^{-2}, reducing the kinetics of both anodic and cathodic reactions, and hence imparting higher protective properties to the composite coating. This effect was previously observed for a pure chitosan coating on stainless steel substrate where the current density was considerably decreased as a result of the chitosan coating.[60] The fact that the second chitosan layer reduces the corrosion potential may be due to its reaction with the media, given chitosan degradation effects. Indeed, degradation of chitosan produces a reduction in the local pH that could increase the tendency to corrode, and therefore, reduces the corrosion potential. However, the potential achieved with the second chitosan layer is in all cases higher than the corrosion potential of the bare material.

As mentioned in the introduction, titanium oxide exhibits biocompatibility as well as antibacterial properties, but, as a ceramic material, it needs to be sintered at high temperatures to increase the adhesion to the substrate. Consequently, hard and rigid coatings are often obtained which may decrease the effective bonding of the implant to the host tissue.[36] As presented in this work, an alternative to the sinter process is the co-deposition of biodegradable polymers, such as polyacrylic acid (PAA), polylactic acid (PLLA), chitosan, *etc.*, with biocompatible inorganic particles (for example: titania, hydroxyapatite or Bioglass®).[64] This new approach leads to soft coatings formed by a hard inorganic particulate material embedded in a compliant polymer matrix which provides suitable adhesion to the substrate avoiding the high temperature sintering step. As a result, a better connection between the implant and bone tissue is anticipated, as a large elastic mismatch at the interface is avoided.

In the last few years, a series of these soft coatings has been electrophoretically obtained by different authors, as summarized recently.[64] For example, TiO_2-containing coatings have been obtained using hyaluronic acid,[61] PAA,[65] PLLA[64] or chitosan[66] as biodegradable polymer matrices. According to Ma *et al.*[61] the thickness of the coatings can be varied from a few nm to 10 μm by adjusting the ceramic content and the deposition time when using hyaluronic acid. The same range of coatings thickness was observed by Wang *et al.*,[65] who showed that the coating thickness can be controlled up to 3 μm by deposition time in the presence of PAA. In our case, the thickness of the n-TiO_2/chitosan coating could be varied from 2 to 6 μm by controlling the ceramic content in the initial colloidal suspension. Thus varying the ceramic content enables the design of the composite composition in order to achieve proper contact angle and corrosion protection properties for possible orthopedic applications of coated metallic

substrates. Indeed EPD can be carried out readily on Ti and Ti alloy substrates.[17] The employment of these coatings in orthopedic applications is also supported by the attractive behavior of chitosan as a biomaterial, which combines the biocompatible properties of the hyaluronic acid[67] with the corrosion protection of PAA[68] and, in addition, provides an antibacterial effect.[69,70]

Conclusions

Novel n-TiO_2/chitosan composite coatings on stainless steel have been successfully obtained by cathodic electrophoretic deposition. The viability of the suspension system has been systematically studied by a trial-and-error approach in terms of dispersant media composition (ethanol–water ratio), voltage and deposition time. The optimal experimental conditions were found to be: an ethanol–water ratio of 80 : 20 (vol.%), in order to avoid bubble formation during EPD and to ensure a high stability of the colloidal suspension, a voltage of 25 V and a deposition time of 1 min. The solid content was also studied using different amounts of n-TiO_2 powder and the "best" coatings, in terms of microstructure homogeneity and substrate adhesion, were those prepared from suspensions containing 1.5 and 3 g L^{-1} n-TiO_2. These coatings have thicknesses of around 2 μm and a ceramic content of 73–84 wt.%. The contact angle of different coatings was also measured resulting in an optimal range (35–80°) for the coating prepared with 1.5 g L^{-1} n-TiO_2 suspensions. The corrosion protection of the coating was tested by electrochemical measurements in DMEM at 37 °C. When using a single layer of the n-TiO_2/chitosan composite, the corrosion protection was found to increase with the ceramic content due to the barrier effect achieved. The addition of a second pure chitosan layer leads to an electrochemical behavior governed by the thickness of the chitosan layer. Further investigation will be carried out to characterize quantitatively the coatings adhesion strength to the substrate in view of applications intended in orthopedic devices and bone tissue engineering scaffolds.

Acknowledgements

L. Cordero-Arias wishes to thank the European Virtual Institute on Knowledge-based Multifunctional Materials (KMM-VIN) for granting a fellowship to visit the Institute of Ceramic Technology (Castellon, Spain) and the German Academic Exchange Service (DAAD) for a scholarship. The authors acknowledge EU ITN FP-7 project "GlaCERCo" for financial support. We thank Dr J. Schmidt (Institute of Particle Technology) and Dr. O. M. Goudouri (Institute of Biomaterials), University of Erlangen-Nuremberg, for experimental support.

References

1 L. Mohan, D. Durgalakshmi, M. Geetha, T. S. N. S. Narayanan and R. Asokamani, *Ceram. Int.*, 2012, **38**, 3435.
2 T. Peltola, M. Patsi, H. Rahiala, I. Kangasniemi and A. Yli-Urpo, *J. Biomed. Mater. Res.*, 1998, **41**, 504.
3 M. J. Santillán, N. E. Quaranta and A. R. Boccaccini, *Surf. Coat. Technol.*, 2010, **205**, 2562.
4 D. Y. Kim, M. Kim, H. E. Kim, Y. H. Koh, H. W. Kim and J. H. Jang, *Acta Biomater.*, 2009, **5**, 2196.
5 P. Evans and D. W. Sheel, *Surf. Coat. Technol.*, 2007, **201**, 9319.
6 Y. Bai, I. S. Park, S. J. Lee, T. S. Bae, W. Duncan, M. Swain and M. H. Lee, *Appl. Surf. Sci.*, 2011, **257**, 7010.
7 X. Nie, A. Leyland and A. Matthews, *Surf. Coat. Technol.*, 2000, **125**, 407.
8 L. X. Zhang, X. L. Wang, P. Liu and Z. X. Su, *Appl. Surf. Sci.*, 2008, **254**, 1771.
9 T. Matsunaga, R. Tomoda, T. Nakajima and H. Wake, *FEMS Microbiol. Lett.*, 1985, **29**, 211.
10 T. Kokubo, H. M. Kim and M. Kawashita, *Biomaterials*, 2003, **24**, 2161.
11 B. Yang, M. Uchida, H. M. Kim, X. Zhang and T. Kokubo, *Biomaterials*, 2004, **25**, 1003.
12 W. H. Song, Y.-K. Jun, Y. Han and S. H. Hong, *Biomaterials*, 2004, **25**, 3341.
13 M. Long and H. J. Rack, *Biomaterials*, 1998, **19**, 1621.
14 M. Navarro, A. Michiardi, O. Castaño and J. A. Planell, *J. R. Soc. Interface*, 2008, **5**, 1137.
15 K. Sunada, Y. Kikuchi, K. Hashimoto and A. Fujishima, *Environ. Sci. Technol.*, 1998, **32**, 726.
16 C. Cui, H. Liu, Y. Li, J. Sun, R. Wang and S. Liu, *Mater. Lett.*, 2005, **59**, 3144.
17 A. R. Boccaccini, S. Keim, R. Ma, Y. Li and I. Zhitomirsky, *J. R. Soc. Interface*, 2010, **7**, S581.
18 R. S. Lima and B. R. Marple, *Mater. Sci. Eng., A*, 2005, **395**, 269.
19 R. Tomaszek, L. Pawlowski, L. Gengembre, J. Laureyns, Z. Znamirowski and J. Zdanowski, *Surf. Coat. Technol.*, 2006, **201**, 45.
20 P. Shi, W. F. Ng, M. H. Wong and F. T. Cheng, *J. Alloys Compd.*, 2009, **469**, 286.
21 H. Farnoush, J. Aghazadeh Mohandesi, D. Haghshenas Fatmehsari and F. Moztarzadeh, *Ceram. Int.*, 2012, **38**, 6753.
22 A. Chávez-Valdez, M. Herrmann and A. R. Boccaccini, *J. Colloid Interface Sci.*, 2012, **375**, 102.
23 Y. Sun and I. Zhitomirsky, *Mater. Lett.*, 2012, **73**, 190.
24 O. O. Van Der Biest and L. J. Vandeperre, *Annu. Rev. Mater. Sci.*, 1999, **29**, 327.
25 I. Corni, M. P. Ryan and A. R. Boccaccini, *J. Eur. Ceram. Soc.*, 2008, **28**, 1353.
26 K. Kanamura and J. Hamagami, *Solid State Ionics*, 2004, **172**, 303.
27 L. Besra and M. Liu, *Prog. Mater. Sci.*, 2007, **52**, 1.
28 A. R. Boccaccini and I. Zhitomirsky, *Curr. Opin. Solid State Mater. Sci.*, 2002, **6**, 251.
29 T. Moskalewicz, A. Czyrska-Filemonowicz and A. R. Boccaccini, *Surf. Coat. Technol.*, 2007, **201**, 7467.
30 C. K. Lin, T. J. Yang, Y. C. Feng, T. T. Tsung and C. Y. Su, *Surf. Coat. Technol.*, 2006, **200**, 3184.
31 S. Dor, S. Rühle, A. Ofir, M. Adler, L. Grinis and A. Zaban, *Colloids Surf., A*, 2009, **342**, 70.
32 W. Tan, X. Yin, X. Zhou, J. Zhang, X. Xiao and Y. Lin, *Electrochim. Acta*, 2009, **54**, 4467.

33 S. Lebrette, C. Pagnoux and P. Abélard, *J. Eur. Ceram. Soc.*, 2006, **26**, 2727.
34 F. Tang, T. Uchikoshi, K. Ozawa and Y. Sakka, *J. Eur. Ceram. Soc.*, 2006, **26**, 1555.
35 D. Hanaor, M. Michelazzi, P. Veronesi, C. Leonelli, M. Romagnoli and C. Sorrell, *J. Eur. Ceram. Soc.*, 2011, **31**, 1041.
36 Z. Zhang, T. Jiang, K. Ma, X. Cai, Y. Zhou and Y. Wang, *J. Mater. Chem.*, 2011, **21**, 7705.
37 N. J. Shah, J. Hong, M. N. Hyder and P. T. Hammond, *Adv. Mater.*, 2012, **24**, 1445.
38 A. W. G. Nijhuis, S. C. G. Leeuwenburgh and J. A. Jansen, *Macromol. Biosci.*, 2010, **10**, 1316.
39 L. Altomare, L. Draghi, R. Chiesa and L. De Nardo, *Mater. Lett.*, 2012, **78**, 18.
40 M. Dash, F. Chiellini, R. M. Ottenbrite and E. Chiellini, *Prog. Polym. Sci.*, 2011, **36**, 981.
41 M. N. R. Kumar, *React. Funct. Polym.*, 2000, **46**, 1.
42 K. Wu, Y. Wang and I. Zhitomirsky, *J. Colloid Interface Sci.*, 2010, **352**, 371.
43 A. Simchi, F. Pishbin and A. R. Boccaccini, *Mater. Lett.*, 2009, **63**, 2253.
44 K. Grandfield and I. Zhitomirsky, *Mater. Charact.*, 2008, **59**, 61.
45 M. Mehdipour and A. Afshar, *Ceram. Int.*, 2012, **38**, 471.
46 X. Pang and I. Zhitomirsky, *Mater. Charact.*, 2007, **58**, 339.
47 F. Pishbin, A. Simchi, M. P. Ryan and A. R. Boccaccini, *Surf. Coat. Technol.*, 2011, **205**, 5260.
48 Y. Cheng, K. M. Gray, L. David, I. Royaud, G. F. Payne and G. W. Rubloff, *Mater. Lett.*, 2012, **87**, 97.
49 K. D. Patel, A. El-Fiqi, H.-H. H.-Y. Lee, R. K. Singh, D.-A. Kim and H.-W. Kim, *J. Mater. Chem.*, 2012, **22**, 24945.
50 Q. Gan and T. Wang, *Colloids Surf., B*, 2007, **59**, 24.
51 R. A. A. Muzzarelli, *Carbohydr. Polym.*, 2011, **83**, 1433.
52 V. R. Sinha, A. K. Singla, S. Wadhawan, R. Kaushik, R. Kumria, K. Bansal and S. Dhawan, *Int. J. Pharm.*, 2004, **274**, 1.
53 F. Sun, X. Pang and I. Zhitomirsky, *J. Mater. Process. Technol.*, 2009, **209**, 1597.
54 K. L. Menzies and L. Jones, *Optometry and Vision Science*, 2010, **87**, 387.
55 J. H. Lee, G. Khang, J. W. Lee and H. B. Lee, *J. Colloid Interface Sci.*, 1998, **205**, 323.
56 A. Pawlak and M. Mucha, *Thermochim. Acta*, 2003, **396**, 153.
57 E. S. Costa-Júnior, M. Pereira and H. Mansur, *J. Mater. Sci.: Mater. Med.*, 2008, **20**, 553.
58 J. Kumirska, M. Czerwicka, Z. Kaczyński, A. Bychowska, K. Brzozowski, J. Thöming and P. Stepnowski, *Mar. Drugs*, 2010, **8**, 1567.
59 W. Khunawattanakul, S. Puttipipatkhachorn, T. Rades and T. Pongjanyakul, *Int. J. Pharm.*, 2010, **393**, 220.
60 F. Gebhardt, S. Seuss, M. C. Turhan, H. Hornberger, S. Virtanen and A. R. Boccaccini, *Mater. Lett.*, 2012, **66**, 302.
61 R. Ma and I. Zhitomirsky, *J. Alloys Compd.*, 2011, **509**, S510.
62 K. Porkodi and S. D. Arokiamary, *Mater. Charact.*, 2007, **58**, 495.
63 C. Q. Ning and Y. Zhou, *Biomaterials*, 2002, **23**, 2909.
64 S. Seuss, A. Chavez, T. Yoshioka, J. Stein and A. R. Boccaccini, *Ceram. Trans.*, 2012, **237**, 145.
65 Y. Wang, I. Deen and I. Zhitomirsky, *J. Colloid Interface Sci.*, 2011, **362**, 367.
66 K. Kavitha, S. Sutha, M. Prabhu, V. Rajendran and T. Jayakumar, *Carbohydr. Polym.*, 2013, **93**, 731.
67 J. B. Leach and C. E. Schmidt, *Biomaterials*, 2005, **26**, 125.
68 E. De Giglio, S. Cometa, N. Cioffi, L. Torsi and L. Sabbatini, *Anal. Bioanal. Chem.*, 2007, **389**, 2055.
69 J. D. Bumgardner, R. Wiser, P. D. Gerard, P. Bergin, B. Chestnutt, M. Marini, V. Ramsey, S. H. Elder and J. A. Gilbert, *J. Biomater. Sci., Polym. Ed.*, 2003, **14**, 423.
70 C. Aimin, H. Chunlin, B. Juliang, Z. Tinyin and D. Zhichao, *Clin. Orthop. Relat. Res.*, 1999, **366**, 239.

